

Original citation:

Cai, Yuanqiang, Xie, Zhiwei, Wang, Jun, Wang, Peng and Geng, Xueyu. (2018) A new approach of vacuum preloading with booster PVDs to improve deep marine clay strata. Canadian Geotechnical Journal .

Permanent WRAP URL:

<http://wrap.warwick.ac.uk/98146>

Copyright and reuse:

The Warwick Research Archive Portal (WRAP) makes this work by researchers of the University of Warwick available open access under the following conditions. Copyright © and all moral rights to the version of the paper presented here belong to the individual author(s) and/or other copyright owners. To the extent reasonable and practicable the material made available in WRAP has been checked for eligibility before being made available.

Copies of full items can be used for personal research or study, educational, or not-for-profit purposes without prior permission or charge. Provided that the authors, title and full bibliographic details are credited, a hyperlink and/or URL is given for the original metadata page and the content is not changed in any way.

Publisher's statement:

Published version: <http://dx.doi.org/10.1139/cgj-2017-0412>

A note on versions:

The version presented here may differ from the published version or, version of record, if you wish to cite this item you are advised to consult the publisher's version. Please see the 'permanent WRAP URL' above for details on accessing the published version and note that access may require a subscription.

For more information, please contact the WRAP Team at: wrap@warwick.ac.uk

20 **Abstract:**

21 This paper presented a new approach for ground improvement of deep marine clay. In
22 which, the conventional booster tube in the current air booster vacuum preloading
23 technology was replaced by the booster PVD. In comparison to the ordinary PVD, the
24 booster PVD could provide inflow channels for the compressed air when the booster
25 pump was in operation. To examine the performance of this new air booster vacuum
26 preloading technology, in-situ field tests were conducted at Oufei sluice project,
27 where the thickness of the soft soil layers (i.e., marine clay) was more than 20 m. An
28 extensive monitoring system was implemented to measure the vacuum pressure, pore
29 water pressure, settlement, and lateral displacement at this reclamation site. With the
30 collected field monitoring data, a comprehensive data analysis was carried out to
31 evaluate the extent of ground improvement. The study results depicted that this new
32 air booster vacuum preloading technology was more effective for the ground
33 improvement of the deep marine clay layers, in comparison to the conventional
34 vacuum preloading technology.

35 **Author keywords:** Land reclamation, Soft clayey soils, Air booster, Vacuum
36 preloading

37 **1 Introduction**

38 Vacuum preloading is one of the well-established technologies for soft ground
39 improvement. It creates negative pressure in the soil through covering the ground
40 surface with an airtight membrane and pumping the air from the soil with
41 prefabricated vertical drains (PVDs). Under the influence of the negative pressure, the
42 water in the pores of the soil moves toward the surfaces via vertical drains,
43 accompanied by a reduction in the pore water pressure and an increase in the effective
44 stress, which thereby promotes the soil consolidation. This technology was first
45 proposed by Kjellman (1952) to improve the subsoils properties of Philadelphia
46 International Airport, USA. From then, a number of scholars have begun to
47 investigate the use of vacuum preloading for the ground improvement of soft soils
48 (Kianfar et al. 2015; Wu et al., 2015; Perera et al. 2016; Wang et al. 2016a; 2016b;
49 2018a; Cai et al. 2017; Fu et al. 2017; 2018; Liu et al. 2017). With these efforts, the
50 vacuum preloading is blossoming into a popular soft ground improvement technology.
51 Nowadays, successful implementations of vacuum preloading technology for ground
52 improvement of the subsoil of airports, railways and highways have been widely
53 reported around the world (e.g., Chu et al. 2000; 2004; 2005a; 2005b; 2006; Shen et
54 al., 2005; Chai et al. 2005; 2006; 2010; Indraratna et al. 2014; Saowapakpiboon et al.
55 2008; Wang et al. 2017; 2018b). In the recent decades, the vacuum preloading
56 technology has also been adopted in the land reclamation where the clay slurry
57 dredged from seabed is used as fill material (Sun et al. 2017; Wang et al. 2016a). In
58 that the untreated soil is oftentimes too soft for the surcharge to be applied, the

59 vacuum preloading technology could be more attractive than the surcharge preloading
60 technology. For example, thousands of hectares of land have been reclaimed in
61 southeastern coastal cities in China with the vacuum preloading technology.

62 The other side of the coin is that the conventional vacuum preloading technology is
63 not free of problems. 1) the blockage of the drainage channel could lead to the
64 reduction of the drainage capacity over elapsed time, in fact, deep soil is more difficult
65 to be further reinforced by longer drainage channels due to clogging; 2) the open style
66 connection of the PVDs in the sand cushion might lead to the excessive dissipation of
67 vacuum pressure, the lower vacuum pressure is not good for the consolidation of soil
68 (Chai and Miura 1999; Bo 2004; Chai et al. 2004). To overcome these issues, an air
69 booster vacuum preloading technology has been proposed (Shen et al. 2011; 2012;
70 2015; Liu et al. 2014). The idea behind this air booster vacuum preloading technology
71 is to apply additional pressure difference between the booster tube and the PVDs, as
72 such the dewatering and consolidation of soil in the late stage of vacuum preloading
73 could be accelerated. In addition, there are some benefits to this technology. Firstly,
74 the compressed air from booster system imposes a flush effect on the fine particles
75 aggregated on the PVDs, which helps mitigate the blockage of the drainage channel
76 and enhance the drainage capacity of the PVDs. Another advantage of this technology
77 is the way of seal connection between tube and PVD. The seal connection of air
78 booster vacuum preloading technology not only can reduce the loss of vacuum during
79 the long-time operation but remove the corresponding cost of the sand cushion.
80 Further, an extra effect of the technology can greatly shorten preloading time and

81 improve the degree of consolidation of soil.

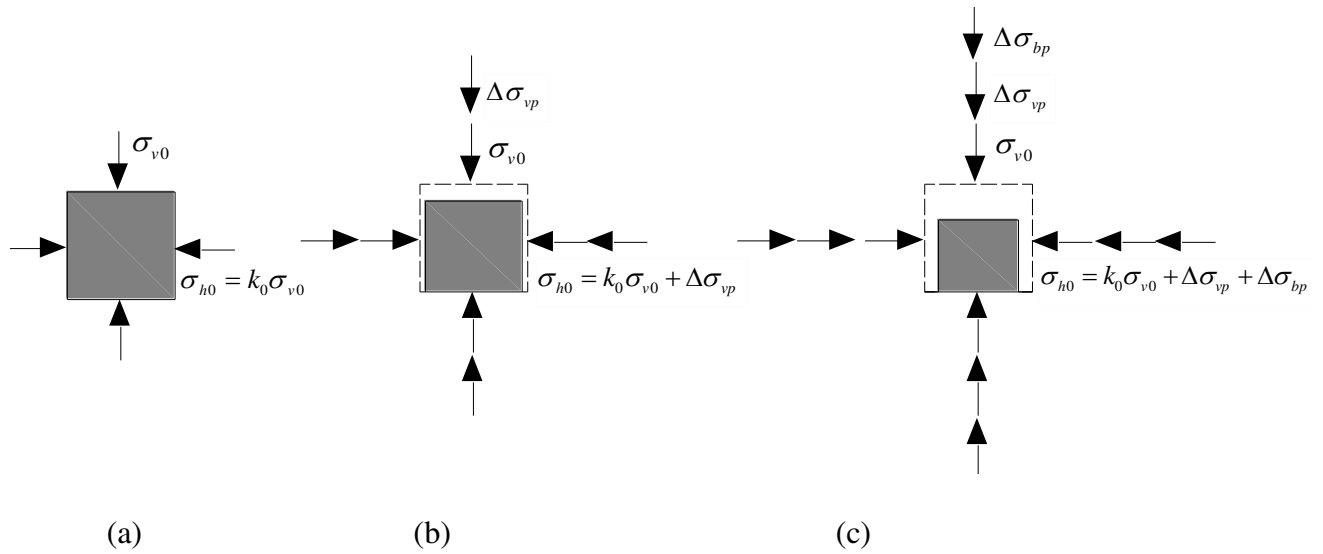
82 Verifications of the air booster vacuum preloading technology have been carried out
83 via in-situ field tests and it has been shown that a more rapid improvement in the soils
84 parameters could be achieved with this technology (Shen et al. 2015; Ding et al. 2015;
85 Wang et al. 2016). It is worth noting that the booster tubes which are made of flexible
86 brackets and filter clothes can only be inserted into a depth of 5 m with manpower and
87 a maximum depth of 8 m with the high pressure water jet; thus, the use of the booster
88 vacuum preloading technology in the ground improvement of deep soft soil might be
89 limited. However, the soft clayey subsoil with a depth of 20 m could be widely
90 encountered in practice. This potential limitation of the air booster vacuum preloading
91 technology therefore necessitates the modification or improvement.

92 In this study, an improved air booster vacuum preloading technology is proposed for
93 the ground improvement of deep marine clay. The major improvement is the
94 dual-functional PVD (termed as booster PVD), which can be easily inserted into the
95 deep marine clay without special equipment and efforts. Part of the booster PVD
96 could provide an inflow channel for the compressed air when the booster pump is
97 activated; otherwise, it plays as an ordinary PVD providing the outflow channel for
98 the air and water. In-situ field tests were conducted to examine the performance of the
99 improved air booster vacuum preloading technology; in which, an extensive
100 monitoring system was implemented to measure the vacuum pressure, pore water
101 pressure, settlement and lateral displacement. With of the field monitoring data, a
102 comprehensive data analysis was carried out to evaluate the extent of soil

103 improvement, and through which the significance of the improved air booster vacuum
104 preloading technology could be demonstrated.

105 **2 Improved air booster vacuum preloading technology**

106 Fig. 1 illustrates the stress states of the soil element during the air booster
107 vacuum preloading process. Initially, the soil element is in an equilibrium state under
108 the actions of the in-situ vertical stress σ_{v0} and horizontal stress σ_{h0} , as shown in Fig.
109 1(a). By applying a vacuum pressure, as shown in Fig. 1(b), the soil element will be
110 subjected to an additional isotropic incremental stress $\Delta\sigma_{vp}$. The soil element trends to
111 consolidate under the incremental stress accompanied with the deformations of the
112 vertical settlement and the inward lateral displacement. As the vacuum preloading
113 proceeds, the consolidation of the soil element under the vacuum pressure fulfills
114 gradually. Next, the booster system is activated and a booster pressure is imposed on
115 the soil element. As shown in Fig. 1(c), the soil element further gains an incremental
116 stress $\Delta\sigma_{bp}$ and thereby undergoes more compressive deformations, which promotes
117 the consolidation of the soil element. During boosting process, the soil will be
118 disturbed by booster airflow. The disturbance will destroy the micro-structure of the
119 soil but only the disturbance will not reduce the void ratio of a soil. It is after the
120 disturbance, the soil particles will try to reach a new steady state and the void ratio
121 will be reduced due to "disturbances induce consolidation (Azari. et al. 2016; Yu. et al.
122 2009; Haeri. et al. 2016) In addition, more cracks will also generate due to the
123 disturbance of airflow. The cracks shorten the seepage path of water in soil void,
124 which promotes the dissipation of the water and thereby accelerates the consolidation
125 of the soil.



128 Fig. 1. Stress state of the soil element subjected to vacuum pressure and booster

129 pressure: (a) initial stress state; (b) stress state under vacuum pressure; (c) stress state
 130 under vacuum pressure and booster pressure

131 In the later period of the consolidation, the scouring influence of airflow of booster
 132 system can effectively alleviate the problem of clogging of PVDs. In booster PVDs,
 133 the function of booster PVDs will be altered from draining to air boosting because of
 134 the activation of the booster system. The pressure difference between booster PVD
 135 and PVD will keep squeezing the soil between them to promote drainage, then the
 136 discharge water also scour the PVD to take away the fine particles of clogging. In
 137 addition, the airflow from the booster pump could wash the booster PVD's drainage
 138 channel and filter jacket directly to allow them to operate more smoothly. Meanwhile,
 139 the airflow in soil will continue to discharge through the PVDs under the vacuum
 140 pressure, and it also plays a role of wash PVD in this process. These functions directly
 141 promote the drainage capacity of PVD, and thus indirect enhance the degree of
 142 consolidation of the soil.

143 As mentioned above, one of the main limitations that prevent the successful
144 implementation of the air booster vacuum preloading technology, in the site
145 applications, is the small embedment depth of the booster tube. Fig. 2 (a) shows the
146 picture of a booster tube which is conventionally used in the air booster vacuum
147 preloading technology. The booster tube is composed of permeable tube segments
148 connected in series by threaded joints, which are made of spiral flexible brackets and
149 filter clothes. Because of the small stiffness, the booster tube can only be embedded
150 into a maximum depth of 8 m even with the aid of the high pressure water jet. This
151 embedment depth is certainly not sufficient for the site applications of soil
152 reinforcement in the southeastern coastal areas of China, where the depth of the soft
153 clay could be as large as 20 m. Note that although the PVDs in the conventional
154 vacuum preloading technology only serve as the outflow channels of the water in the
155 soil, they could certainly perform as the inflow channels of compressed air in the air
156 booster vacuum preloading technology. Thus, the authors proposed the use of PVDs
157 to replace the booster tubes such that the air booster vacuum preloading technology
158 could be applied to the sluice site applications of soil reinforcement. By replacing the
159 booster tubes with booster PVDs (shown in Fig 2b), the small embedment depth of
160 the booster tube can be solved without any additional efforts, as the booster PVD can
161 be inserted into the same depth without any additional effort comparing the ordinary
162 PVD. Here, the booster PVD is designed with dual functions: part of the booster tube
163 could provide the inflow channel of the compressed air when the booster pump is
164 activated; otherwise, the booster tube only plays as an ordinary PVD, providing the

165 outflow channel of the air and water in the soil.



166

167

(a)

(b)

168 Fig. 2. Illustration of the booster pipeline (a) conventional tube and (b) booster PVD

169 Fig. 3 presents a schematic layout of the improved air booster vacuum preloading

170 system. The PVDs are arranged in equilateral triangle grids. The PVD at the center of

171 a hexagon acts as a booster PVD while the adjacent six PVDs serve as ordinary PVDs.

172 The distance between the adjacent PVDs is determined by their effective radius of

173 influence. According to the theories of the consolidation of a unit cell (Biot's. 1941;

174 Onouse. 1988; Yoshikuni and Nakanodo. 1974; Rixner et al. 1986; Chai and Miura.

175 1999; Chai et al. 2011), i.e., a cylinder of soil surrounding a single vertical drain, the

176 effective radius of influence can be estimated as

177 [1]
$$r_e = (15 \sim 22)r_w$$

178 where r_e is the effective radius of influence of the unit cell; and r_w is the equivalent

179 drain radius of a band-shaped PVD, which can be obtained as

180 [2]
$$r_w = \frac{(a+b)}{4}$$

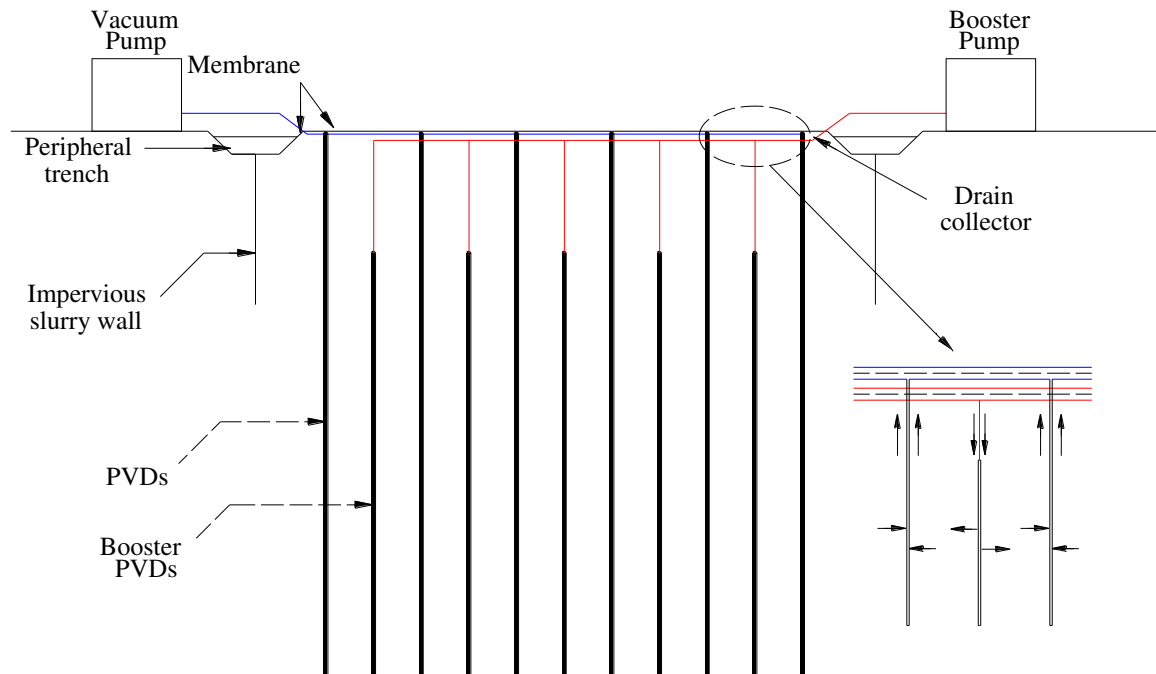
181 where a and b are the width and thickness of the PVD, respectively. With the

182 equal area principle, the radius of the unit cell in a triangular layout can be calculated

183 as

184 [3]
$$r = 0.525S$$

185 where S is the spacing between the adjacent PVDs. By setting $r_e = r$, the spacing
186 between the adjacent PVDs can be determined. The embed depth of the PVDs is
187 mainly dependent on the original properties of the soil as well as the demanded
188 properties of the soil. And both the ordinary and booster PVDs are embedded into the
189 soil with the help of pile equipment.



190

191 Fig. 3. Schematic layout of the improved air booster vacuum preloading system

192 On the ground surface, horizontal drains are placed between two adjacent rows of
193 PVDs, which are connected with the ordinary PVDs at the two sides of the vacuum
194 pump. In addition, horizontal booster pipes are laid out between two adjacent rows of
195 PVDs to link the booster PVDs at the two sides to the vacuum pump or air
196 compressor. To avoid the leakage of compressed air to the ground surface, imporous
197 hose is employed to replace the booster PVD in the shallow soil layer (i.e., no less

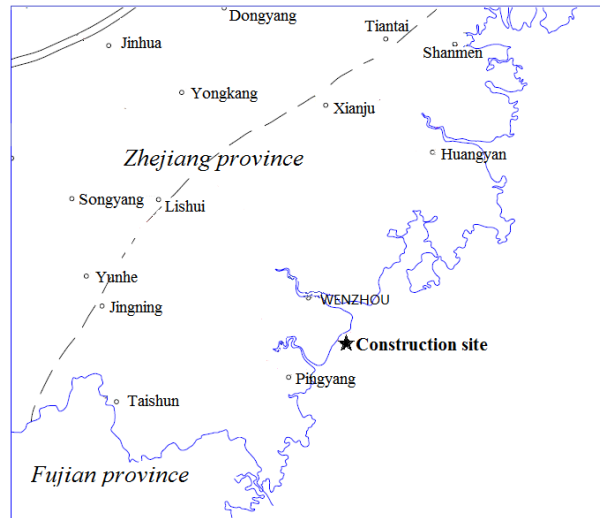
198 than 1 m). The imporous hose is linked to the booster PVD at one end of hose via
199 hand connector and to the horizontal booster pipe at the other end via T joint. Because
200 of the adopted airtight connections, the sand blanket which is usually laid on the
201 ground surface in conventional vacuum preloading technology is no more required in
202 the improved air booster vacuum preloading technology. To seal the area to be
203 improved, two layers of geomembrane are covered on the ground surface, and the
204 geomembrane is anchored into a trench and sealed off with a clay revetment.

205 **3 In-situ field tests**

206 ***3.1 Site conditions***

207 To examine the performance of the improved air booster vacuum preloading
208 technology, in-situ field tests have been carried out at Oufei sluice project in
209 Wenzhou, China. Fig. 4 depicts the planning map of this project. It is the largest
210 individual tideland reclamation program implemented in China, through which a total
211 area of 323.4 km² from the Eastern Sea belt of China in between the estuaries of the Ou
212 River and the Feiyun River will be reclaimed. At the testing site, a sluice gate will be
213 built upon the completion of the ground improvement. The detailed soil profiles at
214 both Zones A and B are presented in Fig. 5. It can be seen from Fig. 5 that the soil
215 profile and properties at Zones A and B are differ slightly, and the marine soil is
216 mainly composed of silt, silt clay, silty clay and muddy-silty clay. The basic soil
217 properties, including the liquid limit (w_L), plastic limit (w_p), water content (w),
218 specific gravity (G_s), void ratio (e_0) and vane shear strength (C_u) are summarized in
219 Table 1. In addition, due to the poor engineering properties of marine soil at the site

220 (high water content and high compressibility), the bearing capacity has to be
 221 improved.



222

223 Fig. 4. Location of the test site in Wenzhou, Zhejiang province, China

224 Table1. Physical and mechanical properties in each soil region

Depth	Water content	Void ratio	Vane shear strength	Liquid limit	Plastic limit	Description of soil
m	%	-	kPa	%	%	-
1.4-1.7	49.6-51.5	1.44-1.85	13.67-18.5	47.1-48.6	22.4-24.3	Silt
5-5.5	55.2-58.5	1.45-1.55	18.5-19.7	42.9-48.5	22.4-24.2	Muddy-silty clay
10-10.3	47.3-53.4	1.16-1.25	23.65-25.36	38.6-41.1	21-21.9	Silt clay
15-15.3	49.9-53.4	1.55-1.56	21.56-23.25	45.2-46.4	23.1-23.5	Silt clay
20-20.3	50.8-51.1	1.62-1.69	23.3-23.88	48-48.3	24-24.1	silt

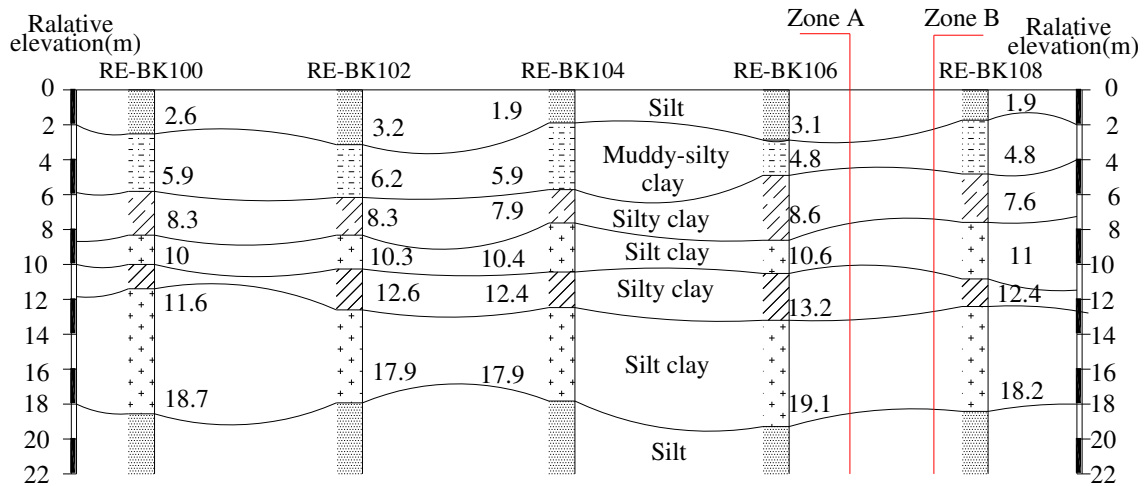
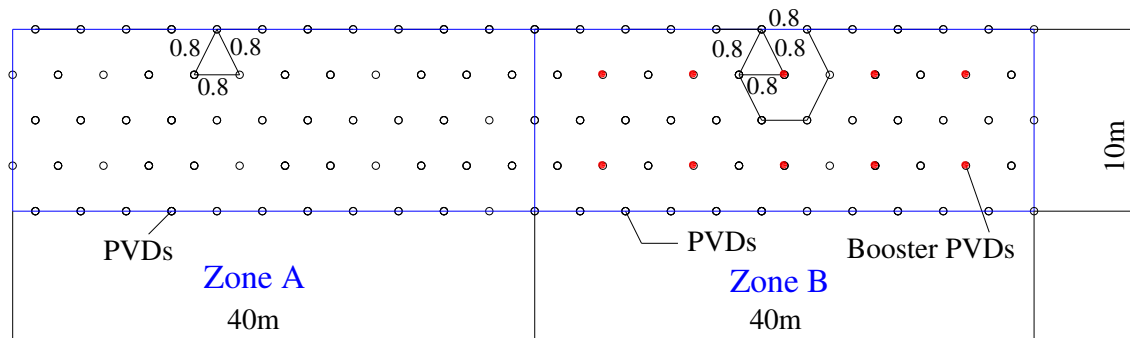


Fig. 5. Subsurface conditions for Oufei land reclamation site

3.2 Soil improvement procedure

To provide a baseline for comparison, the conventional vacuum preloading technology was also tested at the testing site; as such the testing site was divided into two zones, as shown in Fig 6. In Zone A, the conventional vacuum preloading technology was tested. In zone B, the improved air booster vacuum preloading technology was tested. The size of each zone is 40 m by 10 m, and the two zones are separated by an isolation ditch of 1.5 m deep. Because of a sluice gate will be built at the testing site after the completion of the soil improvement, and the sluice gate will subject to horizontal and vertical loads. Therefore, the requirement of depth of soil reinforcement is higher. According to relative engineering experience (Han et al. 2012; Li et al. 2011; Li et al. 2014), the depth of improved area by PVDs is determined using the influence depth of superstructure loading.



239

240

Fig. 6. Layout of in-situ test site

241

The implementation of the improved air booster vacuum preloading technology was

242

elaborated as follows. Off-the-shelf PVDs were employed in this study, which were

243

100 mm in width and 4 mm in thickness, resulting in an equivalent drain radius of 26

244

mm. In reference to Eq (1) and (3), the spacing between the adjacent PVDs was

245

estimated to fall in a range of 742-1090 mm. In order to ensure that the soil can be

246

better reinforced, the spacing between the adjacent PVDs was determined as 800 mm.

247

Hitherto, an improved air booster vacuum preloading system was then installed as it

248

was prescribed in Section 2. As the marine soil was too soft to support the system

249

installation activities, a layer of geotextile was first laid on the ground surface. Upon

250

the completion of the air booster vacuum preloading system, the vacuum system was

251

activated. A vacuum pressure of 85 kPa was applied and maintained using jet pumps

252

with a power of 7.5 kW. In the first stage, the booster PVDs were connected to the jet

253

pumps and thereby functioned as ordinary PVDs. for the first stage lasted 72 days, no

254

notable dissipations of the pore water pressure were observed in deep layers, implying

255

that the discharge capacity of the PVDs was greatly degraded. In the second stage, the

256

booster system was activated through connecting the booster PVDs to the booster

257

pump, and a positive pressure of 20 kPa was selected in this study. This positive

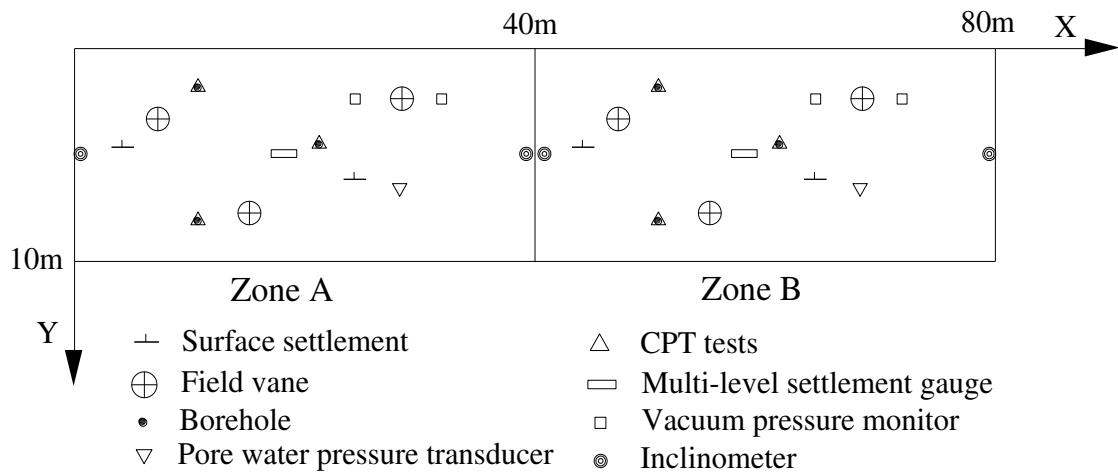
258 pressure was generated by the booster pump with a power of 2.5 kW. It worked 2h/day
259 till the end of the preloading. In addition to 2hour of booster time, the booster PVD is
260 still used to drainage at other times. The preloading was terminated as the following
261 two requirements were both satisfied: 1) the average settlement was less than 2
262 mm/day for a consecutive 5 days; and 2) the dissipation of pore pressure was less than
263 0.02 kPa/day for a consecutive 5 days. In this study, the preloading was terminated
264 after 92 day.

265 The ground improvement procedure in zone A was similar to that in Zone B, except
266 that the air booster system was adopted. In the conventional vacuum preloading
267 system, the horizontal drains are formed by two kinds of pipes, that is, main pipes and
268 branch pipes. The branch pipes were laid horizontally to link the PVDs to the main
269 pipes, which were then connected to the jet pumps. Corrugated flexible pipes with 100
270 mm in diameter were used as horizontal pipes. They were perforated and wrapped with
271 a permeable fabric textile, which served as a filter layer. To transfer the vacuum
272 pressure to the PVDs, a layer of sand blanket with a thickness of 0.5 m was laid on the
273 top of the horizontal drains. The test was also terminated after 92 days.

274 ***3.3 Field monitoring system***

275 To evaluate the extent of the ground improvement, a comprehensive monitoring
276 system was designed to record the vacuum pressure, pore water pressure, settlement,
277 and lateral displacement. Fig. 7 shows the layout of the monitoring system. In each
278 zone, two sets of syringe needles were employed to monitor the vacuum pressure in
279 the PVDs. Three syringe needles were equally distributed in the upper 2 m of the

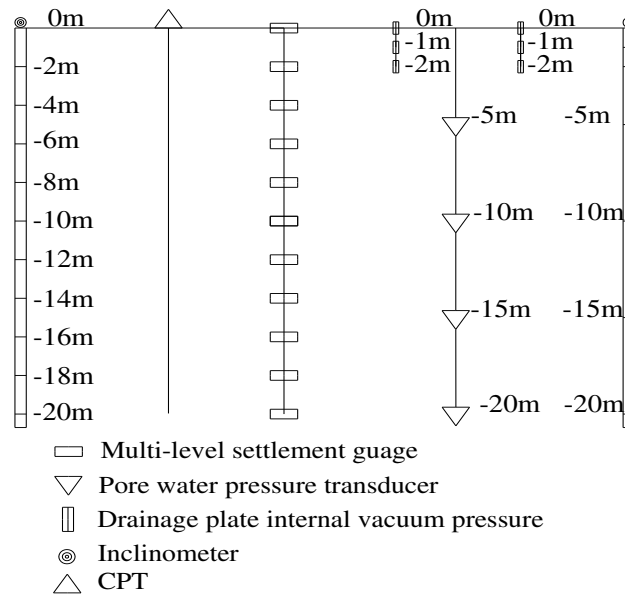
280 PVDs in each set. Four pore water pressure transducers were installed for the
 281 monitoring the pore water pressure at the depth of 5, 10, 15 and 20 m, respectively. A
 282 multi-level settlement gauge was utilized to record the layered settlement; and two
 283 settlement plates were used to measure the surface settlement. One inclinometer was
 284 placed at each side of the zone for monitoring the lateral displacement. In addition,
 285 field vane shear tests and cone penetration tests were performed before and after the
 286 ground improvement. Soil samples within a radial distance of 10 cm to 30 cm from the
 287 PVDs were collected for the laboratory tests.



288

289

(a) Plan view



(b) Elevation view

Fig. 7. Layout of the installed instruments: (a) Plan view and (b) Elevation view

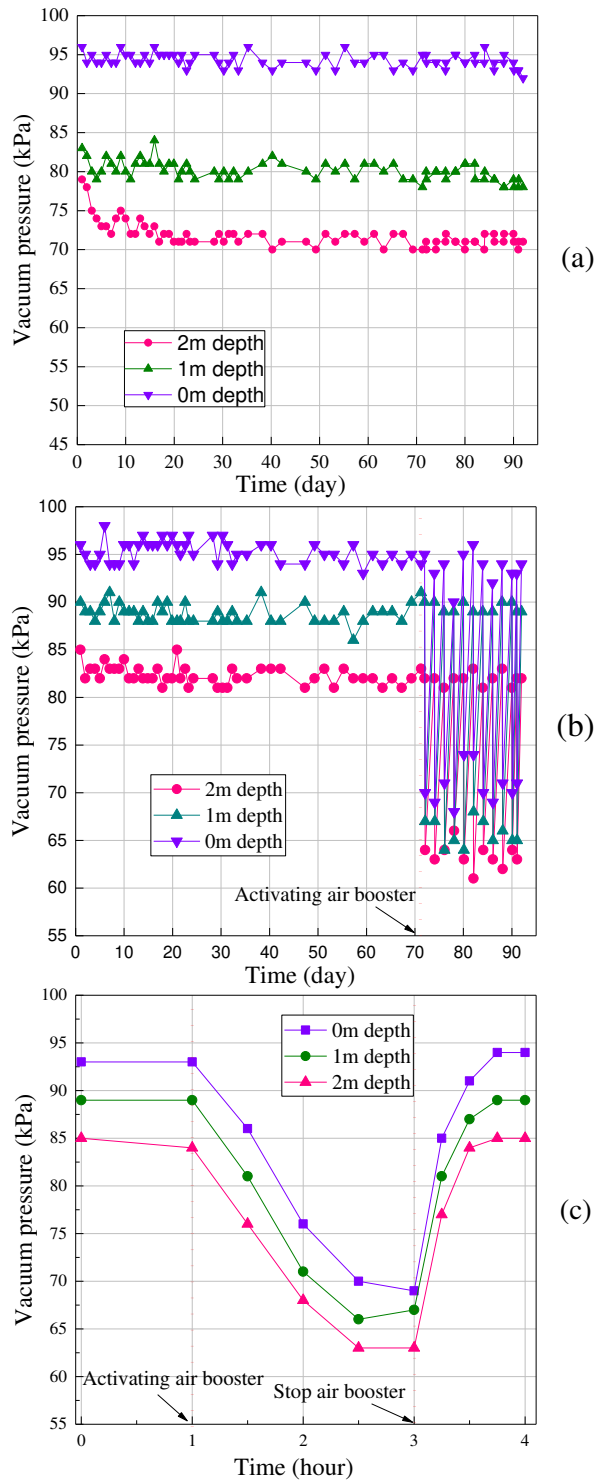
4 Results and discussions

4.1 Vacuum pressure

Fig. 8 shows the distribution of vacuum pressure in the PVDs for the two zones. In Zone A, where the conventional vacuum preloading technology was implemented, notable decrease in the vacuum pressure was observed along the depth and the vacuum loss was much more apparent in the shallow layer, as shown in Fig. 8(a). For example, the vacuum gradient was 15 kPa/m in the upper 1 m, whereas the vacuum gradient was about 8 kPa/m in the depth of 1 m to 2 m. This observation might be attributed to the poor vacuum transmission of the sand blanket covered on the ground surface. Throughout the test, the vacuum pressure remained almost stable and only small fluctuations could be identified at each individual depth.

In Zone B, where the improved air booster vacuum preloading technology was implemented, the decrease in the vacuum pressure along the depth was also observed,

306 as shown in Fig. 8(b). Because of the airtight connections adopted in the improved air
307 booster vacuum preloading technology, the vacuum loss along the depth was smaller
308 in Zone B. For example, the average vacuum pressure over the first 72 days (without
309 booster system) was 82 kPa at the depth of 2 m in Zone B, whereas that was only 72
310 kPa in Zone A. Further the vacuum loss along the depth was more uniform in Zone B.
311 For example, the vacuum gradient was 6 kPa/m in average in the upper 2 m. The
312 vacuum pressure in Zone B maintained stable before the activation of the booster
313 system; however, this vacuum pressure experienced large fluctuations when the
314 booster system was activated. Fig. 8(c) shows the change of vacuum pressure during
315 boosting on the first day of the activation of the booster system. Once the booster
316 system was activated, the vacuum pressure dropped quickly in the first 1.5 hours; after
317 that, the vacuum pressure tended to be stable with small fluctuations. As such, the
318 booster system was turned off after 2 hours. Upon the shutdown of the booster system,
319 the vacuum pressure recovered rapidly to the state before the pressurization within half
320 an hour.



321

322 Fig. 8. Variations in the vacuum pressure in PVDs: (a) in zone A; (b) in zone B; (c) on

323 the first day of the activation of the booster system in zone B

324 4.2 Pore water pressure

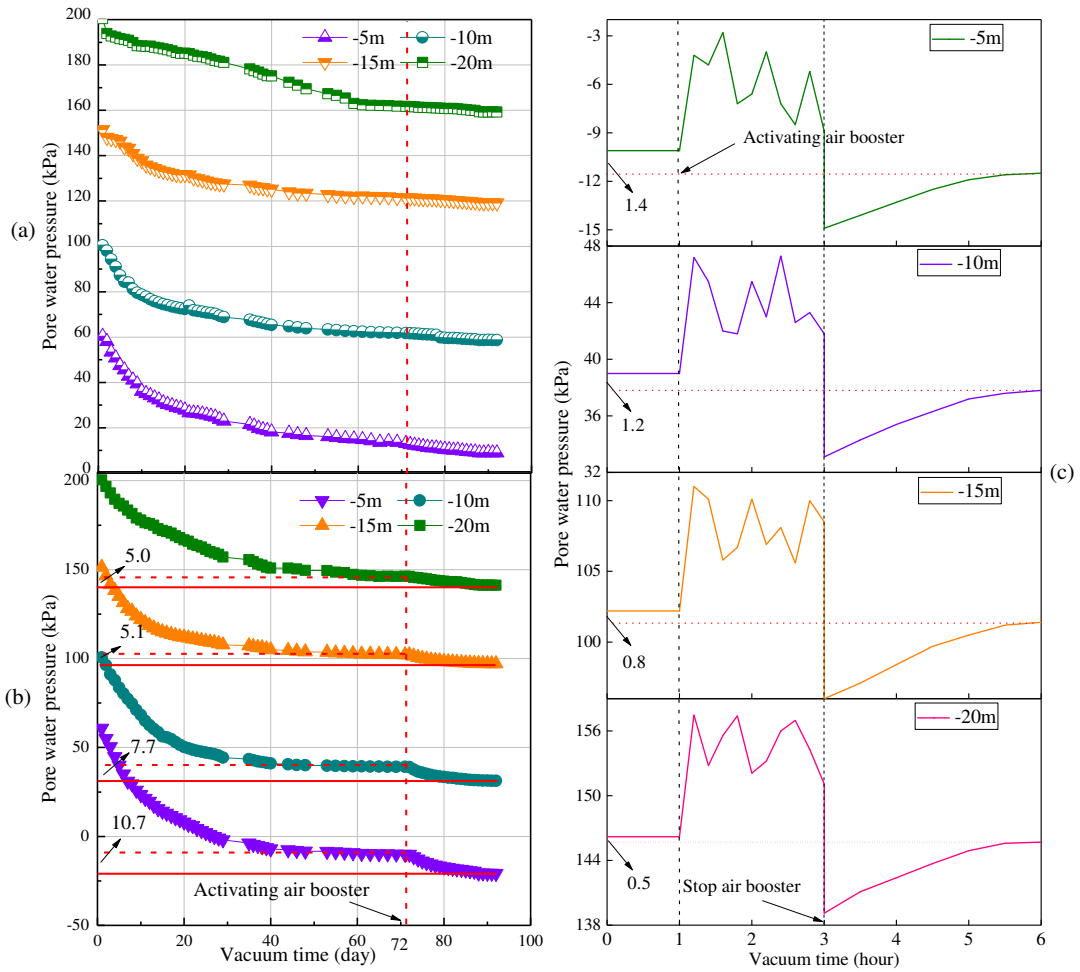
325 Fig. 9 shows the distribution of the monitored pore water pressure in the soil for the

326 two zones. The plots in Fig. 9(a) show a rapid dissipation of the pore water pressure at
327 the beginning of the preloading in Zone A. For example, the pore water pressure was
328 dropped by 32.6 kPa, 28 kPa, 19.8kPa and 15.2kPa at the depth of 5 m, 10m, 15m and
329 20m, respectively, in the first 20 days, accounting for 63%, 67%, 61% and 37% of the
330 total pore water pressure dissipated at the end of the preloading. Because of the
331 vacuum loss along the depth, the dissipation rate of the pore water pressure decreased
332 along the depth in the early stage. As the test proceeded, the dissipation of pore water
333 pressure slowed down gradually and the difference in the dissipation rate along the
334 depth became negligible. After 72 days of preloading, the dissipation rate of the pore
335 water pressure decreased to less than 0.05 kPa/day at all depths. At the end of the test,
336 the pore water pressure was decreased by 51.4 kPa, 41.7 kPa, 32.4 kPa and 41.2 kPa
337 at the depth of 5m, 10m, 15m and 20m, respectively. It is noted that the dissipation of
338 pore water pressure at the depth of 20 m is larger than the counterpart at the depth of
339 15 m, which might be interpreted by the following fact: the silt clay at the depth of 15
340 m causes more severe congestion in the PVDs than the silt at the depth of 20 m.

341 The dissipation of the pore water pressure in Zone B was similar to that in Zone A
342 before the activation of the booster system, as shown in Fig. 9(b). Because of the
343 larger vacuum pressure induced by the airtight connection technology, the dissipation
344 of pore water pressure in Zone B was much faster in the early stage of this test. After
345 72 days' of preloading, the difference between the pore water pressures in the two
346 zones accumulated up to 23.1 kPa, 23.0 kPa, 19.0 kPa and 15.4 kPa at the depth of 5 m,
347 10 m, 15 m and 20 m, respectively. In other words, the dissipation of the pore water

348 pressure in zone B at the depth of 5 m, 10 m, 15 m and 20 m was increased by 48%,
349 59%, 63% and 40%, respectively, in comparison to those in Zone A. Further, notable
350 decreases were observed in the pore water pressure in Zone B after the activation of
351 the booster system. With the aid of the booster system, the pore water pressure was
352 further decreased by 10.7 kPa, 7.7 kPa, 5.1 kPa and 5 kPa at the depth of 5 m, 10 m,
353 15 m and 20 m, respectively. It is worth noting that the reduction in the pore water
354 pressure was also apparent in the deep soil layer. For example, the pore water pressure
355 dissipated in the last 20 days could account for 8.4% of the total dissipation of the
356 pore water pressure at the depth of 20 m. It demonstrates that the improved air booster
357 vacuum preloading technology is more effective for promoting the consolidation of
358 the deep soil layer. For example, at the end of the test, the dissipation of pore water
359 pressure in zone B at the depth of 5 m, 10 m, 15 m and 20 m was 58%, 66%, 67% and
360 44% larger than those in Zone A.

361 Fig. 9(c) shows the pore water pressure measured during boosting on the first day of
362 the activation of the booster system. As can be seen, the pore water pressure fluctuated
363 significantly during the pressurization. Finally, the pressurization caused notable
364 reductions in the pore water pressures. For example, the pore water pressure was
365 dropped by 1.4 kPa, 1.2 kPa, 0.8 kPa and 0.5 kPa at the depth of 5, 10, 15 and 20 m,
366 respectively, at the end of the pressurization.



367

368 Fig. 9. Variations in the pore water pressure at different depths: (a) in zone A; (b) in
 369 zone B; (c) on the first day of the activation of the booster system in Zone B

370 **4.3 Degree of consolidation**

371 The average degree of consolidation (DOC) can be calculated from the monitored
 372 pore water pressure. The distribution profiles of the monitored pore water pressure are
 373 illustrated in Fig. 10, with which the average DOC, U_{avg} , can be calculated as follows:

374 [3]
$$U_{avg} = 1 - \frac{\int [u_t(z) - u_s(z)] dz}{\int [u_0(z) - u_s(z)] dz}$$

375 and

376 [4]
$$U_s(z) = \gamma_w z - s(kPa)$$

377 where $u_0(z)$ is the initial pore water pressure at depth z ; $u_t(z)$ is the final pore water
378 pressure at depth z ; $u_s(z)$ is the suction at depth z ; γ_w is the unit weight of water; and
379 s is the applied suction (80 kPa). The integrals in the numerator and denominator of
380 Eq. (4) can be calculated using the area between the curve $u_t(z)$ and the line $u_s(z)$.
381 According to the formulation in Eq. (4), the U_{avg} can be calculated and the results are
382 shown in Fig. 10, the calculated U_{avg} in Zone B was 80% and that in Zone A was 52%.
383 DOC at different time is shown in Table 2. A comparison of the calculated DOC at
384 the elapsed time of 72 days and 92 days indicates that the most contribution is
385 associated with the airtight connection vacuum system. However, Table 2 shows that
386 the increased of DOC in Zone B is greater than that in Zone A during the last 20 days.
387 This table result also supports the statement that the improved air booster vacuum
388 preloading technology accelerates the consolidation of the soil.

389 **Table. 2. Degree of consolidation at different times in both zones**

Time (days)	DOC (Zone A)	DOC (Zone B)
72	49%	74%
92	52%	80%

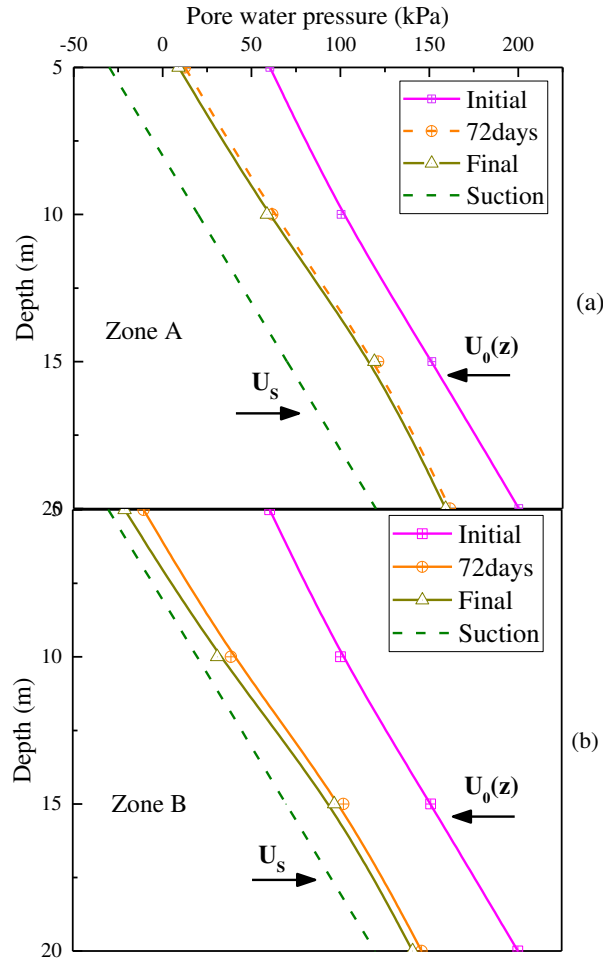
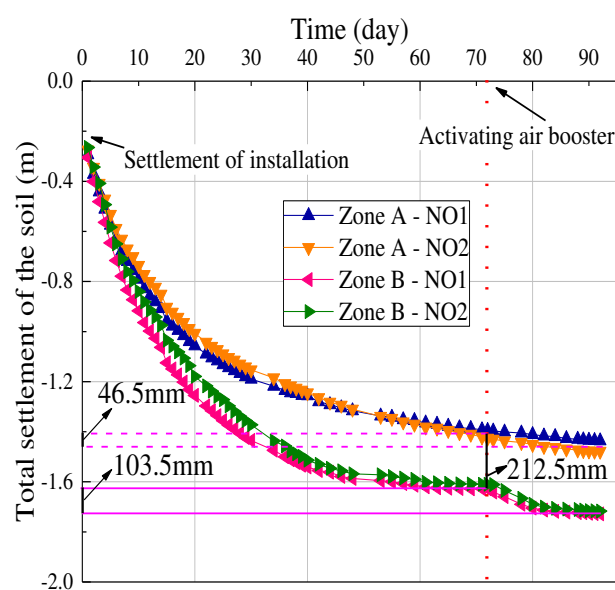


Fig. 10. Pore water pressure distribution with depth: (a) zone A and (b) zone B

4.4 Surface settlement

Fig. 11 presents the evolution of the ground surface settlement in the two zones. At the beginning of the preloading, the surface settlement in zone A was slightly larger than that in zone B. It is attributed to the fact that Zone A was subjected to an additional surcharge which was applied by the 0.5 m thick sand blanket on the ground surface. After the 15 days' preloading, the surface settlement in Zone B, however, began to exceed that in Zone A. As the preloading proceeded, the increase in the surface settlement slowed down in both zones. At the end of 72 days' preloading, the difference between the average surface settlements in the two zones was as large as

401 212.5 mm. Thus, the faster consolidation of the soil was achieved by the improved air
 402 booster vacuum preloading technology. The surface settlement in Zone B tended to
 403 converge before the activation of the booster system, whereas the surface settlement in
 404 zone A did not converge until 85 days. When the booster system in Zone B was
 405 activated, notable increment in the surface settlement occurred. During the boosting
 406 period, the average surface settlement in Zone B was increased by 103.5 mm, which
 407 accounted for 6% of the total surface settlement; in contrast, the average total surface
 408 settlement in Zone A was only increased by 46.5 mm only, accounting for 3% of the
 409 total surface settlement. In other words, the surface settlement accumulated in this
 410 period in Zone B was two times of that in Zone A; and, part of the settlement
 411 difference in the two zones is due to the air-boosting. Thus, the improved air booster
 412 vacuum preloading technology helps accelerate the consolidation of soil. At the end of
 413 the test, the average surface settlement in zone A and zone B was 1457 mm and 1722.5
 414 mm, respectively.

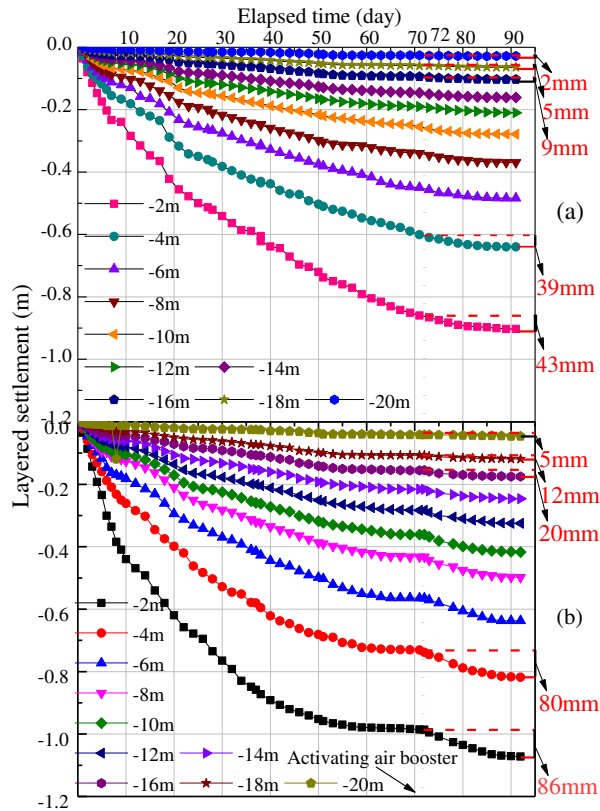


415

416 Fig. 11. Monitored total surface settlements against elapsed time for the two zones

417 **4.5 Layered settlement**

418 Fig. 12 plots the evolution of layered settlement in the two zones. In zone A, the
419 layered settlement increased with decreasing of growth rate as the test proceeded, as
420 shown in Fig. 12(a). In zone B, the evolution of the layered settlement was similar to
421 that in Zone A before the activation of the booster system, as shown in Fig. 12(b).
422 However, the accumulated settlement in zone B was larger than that in zone A, which
423 can be attributed to the airtight connections adopted in the improved air booster
424 vacuum preloading technology. After the activation of the booster system, obvious
425 increment in the layered settlement was found in Zone B. During the last 20 days, the
426 accumulated settlement in Zone B was 86 mm, 80 mm, 20 mm, 12 mm and 5 mm at
427 the depth of 2 m, 4m, 16 m, 18 m and 20 m, respectively; whereas, in the same period,
428 the accumulated settlement in Zone A was only 43 mm, 39 mm, 9 mm, 5 mm and 2
429 mm at the depth of 2 m, 4m, 16 m, 18 m and 20 m, respectively. As can be seen, the
430 accumulated settlement in Zone B during the last 20 days has a significant increase at
431 each layer with the help of a booster system. Thus, the improved air booster vacuum
432 preloading technology is more competent for improving the deep marine clay layers.



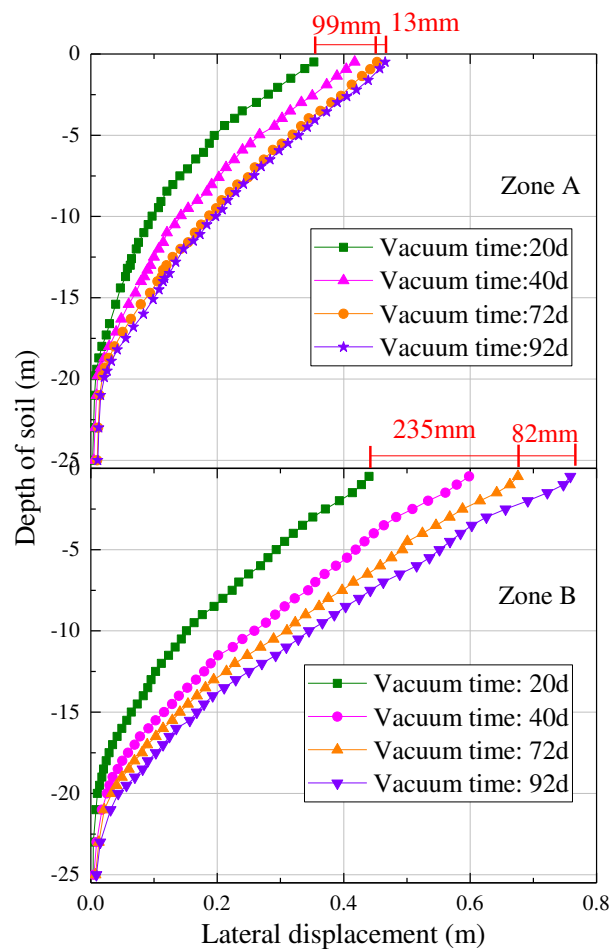
433

434 Fig. 12. Layered settlements measured at different depths during vacuum preloading
 435 against elapsed time: (a) Zone A and (b) Zone B

436 **4.6 Lateral displacement**

437 It is known that a vacuum pressure tends to induce inward displacement (toward the
 438 center of a zone) in the soil, and Fig. 13 presents the profile of the lateral displacement
 439 in the two zones. The plots in Figure 13 indicated the lateral displacements in the two
 440 zones were similar. The lateral displacement gradually decreased with the depth;
 441 however, the lateral displacement in zone A was smaller than that in zone B, especially
 442 in the shallow soil layer. For a deep analysis of the difference in the lateral
 443 displacement between these two zones, the lateral displacement is normalized herein
 444 by the maximum lateral displacement. In Fig. 14, the normalized lateral displacement
 445 at 20 days in Zone B is greater than that in Zone. At the end of 72 days' preloading,
 446 the lateral displacement at the ground surface in Zone B was 675 mm, which was 49%
 447 larger than that in zone A (i.e., 452 mm). When the booster system was activated, the

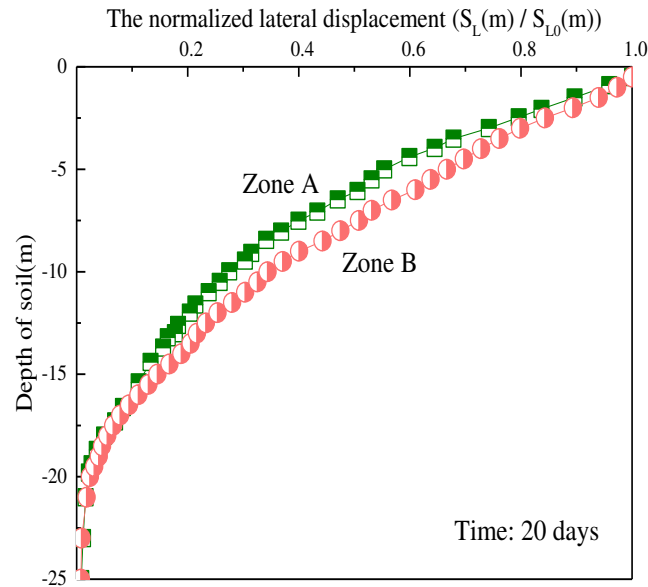
448 lateral displacement at the ground surface in zone B was increased by 82 mm, while it
 449 was only increased by 13 mm in zone A; and, at the end of the test, the lateral
 450 displacement in zone A and zone B was 465 mm and 758 mm, respectively. Test
 451 results indicated that air booster vacuum preloading method can cause more lateral
 452 displacement, and the more lateral displacement means that the soil can get better
 453 compression and consolidation, which are more conducive to the later stage of
 454 engineering construction.



455

456

Fig. 13. Curves of the monitored lateral displacement against elapsed time

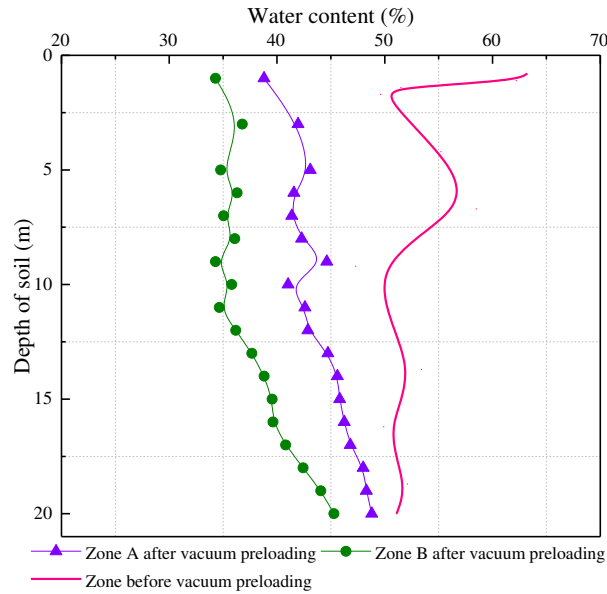


457

458 **Fig. 14. Curves of the normalized lateral displacement against elapsed time in two**
 459 **zones at 20 days**

460 **4.7 Water content**

461 Fig. 15 shows the water content profiles in the two zones. Before the preloading, the
 462 water content was more than 45% within the depth of 20 m, and which was 65% in
 463 the shallow soil layer. After the ground treatment, significant reductions in the water
 464 content were observed in both zones. For example, the water content in the shallow
 465 soil layer was reduced to 38.8% and 34.3% in zone A and Zone B, respectively.
 466 Further, the water content profiles in the two zones were similar in shape and it
 467 generally increased with the depth; however, at a given depth, the water content in
 468 Zone B tended to be smaller than that in Zone A. Here, the average water content in
 469 the deep soil layer (i.g., 15 m~20 m) in zone B was reduced by 10% while that in Zone
 470 A was only reduced by 4%. Thus, the improved air booster vacuum preloading
 471 technology outperformed the conventional vacuum preloading technology in the soft
 472 soil improvement.



473

474

Fig. 15. Measured water content profiles in the initial and final stage

475 **4.8 Vane shear strength**

476 Fig. 16 presents the shear strength profiles in the two zones which are obtained with

477 the vane shear tests. Before the ground improvement, the vane shear strength was less

478 than 25 kPa within the depth of 20 m, and the vane shear strength was as small as 15

479 kPa in the shallow soil layer. After the ground improvement, the vane shear strength

480 in both zones increased significantly. For instance, the vane shear strength in the

481 shallow soil layer was increased to 37.8 kPa and 43.2 kPa in Zone A and Zone B,

482 respectively. The profiles of the vane shear strength in both zones showed the same

483 behavior. In both zones, the shear strength decreases as the depth increases in a

484 general trend. Further, the vane shear strength in Zone B was always larger than that

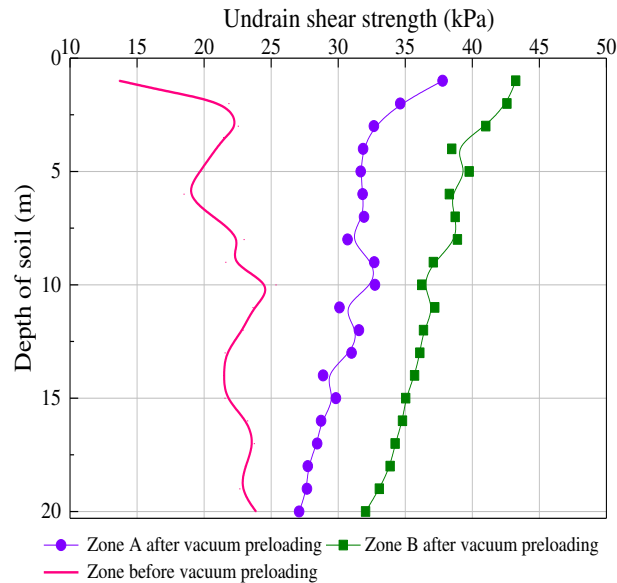
485 in Zone A. Here, notable increment in the vane shear strength in the deep soil layer

486 was also achieved by the improved air booster vacuum preloading technology. For

487 example, the vane shear strength at the depth of 20 m was increased from 23.9 kPa to

488 32.0 kPa in Zone B, while it was only increased to 27.1 kPa in Zone A. Thus, the

489 superiority of the improved air booster vacuum preloading technology was
490 demonstrated.



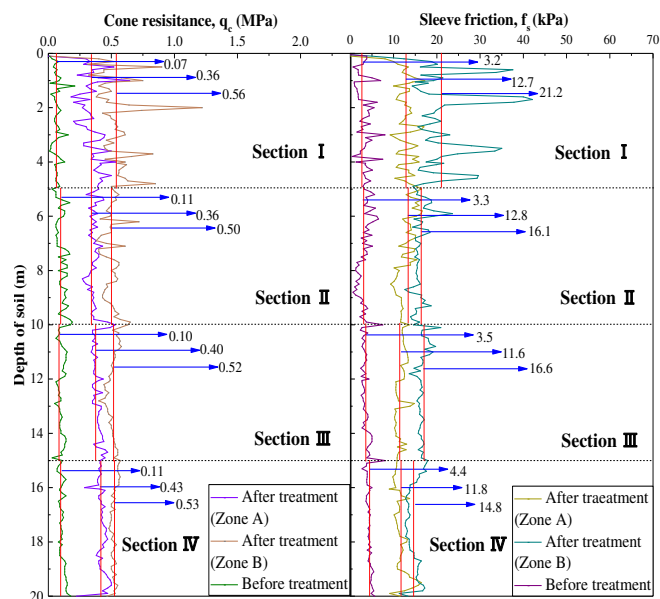
491

492 Fig. 16. Measured field vane shear strength profiles in the initial and final stage

493 **4.9 Cone resistance and sleeve friction**

494 Fig. 17 shows the cone resistance and frictional resistance in the two zones obtained
495 with the cone penetration tests. For better analysis of soil reinforcement at different
496 depths, the soil was divided into four segments along the depth, and the average cone
497 resistance and fictional resistance was calculated for each segment. Before the ground
498 improvement, both cone resistance and sleeve friction resistance were small. Within
499 the depth of 20 m, the cone resistance was smaller than 0.21 MPa and the sleeve
500 friction was smaller than 8.1 kPa. After the ground improvement, both cone resistance
501 and sleeve friction gained significant increases. For example, the average cone
502 resistance in Segment IV was increased from 0.11 MPa to 0.43 MPa in Zone A and
503 0.53 MPa in Zone B; and, the average sleeve friction in Segment IV was increased
504 from 4.4 kPa to 11.8 kPa in Zone A and 14.8 kPa in Zone B. That is to say, both cone

505 resistance and sleeve friction in zone B were larger than those in zone A. The average
 506 cone resistance in the four segments in Zone B was 55%, 39%, 30% and 23% larger
 507 than that in Zone A, and the average sleeve friction in the four segments in Zone B
 508 were 67%, 26%, 43% and 25% larger than that in Zone A. Thus the developed air
 509 booster vacuum preloading technology was more effective than the conventional
 510 vacuum preloading technology.



511

512 Fig. 17. Measured frictional resistance and cone resistance profiles in the initial and
 513 final stage

514 5 Conclusions

515 This study proposed an improved air booster vacuum preloading technology for the
 516 ground improvement of deep marine clay layers, in which the conventional booster
 517 tube was replaced by the booster PVD. In-situ field tests were conducted at Oufei
 518 sluice project to examine the performance of the improved air booster vacuum
 519 preloading technology. A comprehensive monitoring system was implemented to
 520 measure the vacuum pressure, pore water pressure, settlement, and lateral displacement.

521 The analysis of the monitoring data was carried out to evaluate the extent of soil
522 improvement. The major conclusions of this study are as follows:

523 (1) The improved air booster vacuum preloading technology is shown superior to the
524 conventional vacuum preloading technology. For the conventional vacuum preloading,
525 the dissipation of the pore water pressure almost vanished after 72 days within 20m
526 depths. For the air booster vacuum preloading, notable reductions appeared in the
527 pore water pressures after the activation of the booster system, and the pore water
528 pressure dissipation in the deep soil layer was particularly apparent.

529 (2) The improved air booster vacuum preloading technology performs better than the
530 conventional vacuum preloading technology. During last 20 days, the layered
531 settlement generated by the former was more than double the counterpart yielded by
532 the latter.

533 (3) The improved air booster vacuum preloading technology is more competent than
534 the conventional vacuum preloading technology in improving the physical and
535 mechanical properties of the soil. The vane shear strength of the soil enhanced by the
536 former was always larger than its counterpart improved by the latter. Both cone
537 resistance and frictional resistance of the soil achieved by the former were larger than
538 their counterparts by the latter.

539 **Acknowledgements**

540 This research was supported by National Key R&D Program of China
541 (2016YFC0800200), the Program of International Science and Technology
542 Cooperation (No. 2015DFA71550), the National Natural Science Foundation of China

543 (No. 51622810, No. 51778501 and No. 51620105008), the Zhejiang Province Natural
544 Science Foundation of China under Grant No. LR18E080001, and the Key Research
545 and Development Program of Zhejiang Province under Grant No. 2018C03038. This
546 financial support is gratefully acknowledged.

547 **Notation**

548 Basic SI units are shown in parentheses

549 W_L Liquid limit (dimensionless)

550 W_P Plastic limit (dimensionless)

551 W Water content (dimensionless)

552 G_s Specific gravity (dimensionless)

553 e_0 Void ratio (dimensionless)

554 C_u Undrained shear strength (Pa)

555 **References**

Azari, B., Fatahi, B., & Khabbaz, H. 2016. Assessment of the elastic-viscoplastic behavior of soft soils improved with vertical drains capturing reduced shear strength of a disturbed zone. *International Journal of Geomechanics*, 16(1), B4014001-15.

Bo, M.W. 2004. Discharge capacity of prefabricated vertical drain and their field measurements. *Geotextiles & Geomembranes*, **22**(1–2), 37-48.

Biot, M.A. 1941. General theory of three - dimensional consolidation. *J.appl.phys*, **12**(2), 155-164.

Chu, J., Yan, S. W., & Yang, H. 2000. Soil improvement by the vacuum preloading

- method for an oil storage station. *Geotechnique*, **50**(6), 625-632.
- Chu, J., Bo, M.W., & Choa, V. 2004. Practical considerations for using vertical drains in soil improvement projects. *Geotextiles & Geomembranes*, **22**(1-2), 101-117.
- Chu, J., and Yan, S.W. 2005a. Application of the vacuum preloading method in soil improvement projects. In *Ground Improvement - Case Histories*. Edited by I. Buddhima and C. Jian. Elsevier. pp. 91-117.
- Chu, J., & Yan, S.W. 2005b. Estimation of degree of consolidation for vacuum preloading projects. *International Journal of Geomechanics*, **5**(2), 158-165.
- Chu, J., & Yan, S.W. 2006. Effective depth of vacuum preloading. *Lowland Technology International the Official Journal of the International Association of Lowland Technology*, **8**, 1-8.
- Chai, J. C., & Miura, N. 1999. Investigation of factors affecting vertical drain behavior. *Journal of Geotechnical & Geoenvironmental Engineering*, **125**(3), 216-226.
- Chai, J. C., Miura, N., & Nomura, T. 2004. Effect of hydraulic radius on long-term drainage capacity of geosynthetic drains. *Geotextiles & Geomembranes*, **22**(1), 3-16.
- Chai, J.C., Carter, J.P., & Hayashi, S. 2005. Ground deformation induced by vacuum consolidation. *Journal of Geotechnical & Geoenvironmental Engineering*, **131**(12), 1552-1561.
- Chai, J.C., Carter, J.P., & Hayashi, S. 2006. Vacuum consolidation and its combination with embankment loading. *Canadian Geotechnical Journal*, **43**(10), 985-996.
- Chai, J.C., Hong, Z. & Shen, S. 2010. Vacuum-drain consolidation induced pressure

distribution and ground deformation. *Geotextiles and Geomembranes*, 28, No. 6, 525–535.

Chai, J.C., & Carter, J.P. 2011. *Deformation Analysis in Soft Ground Improvement*. Springer Netherlands.

Cai, Y., Qiao, H., Wang, J., Geng, X., Wang, P., Cai, Y., 2017. Experimental tests on effect of deformed prefabricated vertical drains in dredged soil on consolidation via vacuum preloading. *Engineering Geology* 222, 10-19.

Ding, H.L., Guo, Z.P., Fan, K.Y., Wang, Z.T., & Qian, M. 2015. Comparative Experiment on Soft Soil Treatment by Air-boosted Vacuum Preloading. *Chinese Journal of Underground Space and Engineering*. 11(S1): 1673-0836 (in Chinese).

Fu, H.T., Cai, Y.Q., Wang*, J., Wang, P. 2017. Experimental study on the combined application of vacuum preloading-variable-spacing electro-osmosis to soft ground improvement. *Geosynthetics International* . 24(1): 72-81.

Fu, H.T., Fang, Z.Q., Wang*, J., Chai, J.C., Cai, Y.Q., Geng, X.Y., Jin, J.Q. & Jin, F.Y. 2018. Experimental Comparison of Electro-Osmotic Consolidation of Wenzhou Dredged Clay Sediment Using Intermittent Current and Polarity Reversal. *Marine Georesources & Geotechnology*. 36(1):131-138.

Haeri, S. M., Khosravi, A., Garakani, A. A., & Ghazizadeh, S. 2016. Effect of soil structure and disturbance on hydromechanical behavior of collapsible loessial soils. *International Journal of Geomechanics*, 17(1), 04016021.

Han, W. J., Liu, S. Y., Zhang, D. W., & Du, G. (2012). Field Behavior of Jet Grouting

- Pile under Vacuum Preloading of Soft Soils with Deep Sand Layer. Geocongress (pp.70-77).
- Indraratna, B., Rujikiatkamjorn, C., & Balasubramaniam, A.S. 2014. Consolidation of estuarine marine clays for coastal reclamation using vacuum and surcharge loading. *Geotechnical Special Publication*(233), 358-369.
- Kjellman, W. 1952. Consolidation of clayey soils by atmospheric pressure. *Proceedings of a Conference on Soil Stabilization*, Massachusetts Institute of Technology, USA: 258-263.
- Kianfar, K., Indraratna, B., Rujikiatkamjorn, C., & Leroueil, S. 2015. Radial consolidation response upon the application and removal of vacuum and fill loading. *Canadian Geotechnical Journal*, 52(12): 2156-2162
- Liu, H., Yu, X.P., et al. 2014. Comparative experiment study on the strengthening of dredger fill using vacuum preloading method based on pressurization and anti-clogging technology [J]. *Railway standard design*, **58**(1): 28-33 (in Chinese)
- Liu, F.Y., Fu, H.T., Wang*, J., Mi, W. 2017. Influence of soluble salt on electro-osmotic consolidation of soft clay. *Soil Mechanics and Foundation Engineering*. 54(1):49-55
- Li, A. G., Tham, L. G., Wen, J. P., & Chen, S. C. (2014). Case study of ground improvement to qianhai reclamation area, qianhai bay, shenzhen. *Geotechnical Special Publication*(238), 231-240.
- Li, B., Wu, S. F., Chu, J., & Lam, K. P. (2011). Evaluation of Two Vacuum Preloading. *Techniques Using Model Tests. Geo-Frontiers Congress*

(pp.636-645).

Onoue, A. 1988. Consolidation by vertical drains taking well resistance and smear into consideration. *Soils & Foundations*, **28**(4), 165-174.

Perera, D., Indraratna, B., Leroueil, S., Rujikiatkamjorn, C., & Kelly, R. 2016. An analytical model for vacuum consolidation incorporating soil disturbance caused by mandrel-driven drains. *Canadian Geotechnical Journal*.54(4) : 547-560

DOI: 10.1139/cgj-2016-0232

Rixner, J.J., Kraemer, S.R., & Smith, A.D. 1986. Prefabricated vertical drains. volume 2. summary of research effort. Facilities.

Saowapakpiboon, J., Bergado, D.T., Chai, J.C., Kovittayanon, N., & Zwart, T.P.D. 2008. Vacuum-PVD Combination with Embankment Loading Consolidation in Soft Bangkok Clay: A Case Study of the Suvarnabhumi Airport Project. *Geosynthetics in Civil and Environmental Engineering*. Springer Berlin Heidelberg.

Shen, S.L, Chai, J.C., Hong, Z-S., and Cai, F.X. 2005. Analysis of field performance of embankments on soft clay deposit with and without PVD-improvement, *Geotextiles and Geomembranes*, 23(6), 463-485.

Shen, Y.P., Yu, J., Liu, H., & Li, Z. 2011. Experiment study on air-boosted vacuum preloading of soft station foundation [J]. *Journal of the China Railway Society*, **33** (5): 97-103. (in Chinese)

Shen, Y.P., Feng, R.L., Zhong, S.Y., & Li, Z. 2012. Study on optimized design of vacuum preloading with air pressure boosted for treatment of railway station &

- yard foundation [J]. *Journal of the China railway society*, **34** (4): 88-93. (in Chinese)
- Shen, Y., Wang, H., Tian, Y., Feng, R., Liu, J., & Wu, L. 2015. A new approach to improve soft ground in a railway station applying air-boosted vacuum preloading. *Geotechnical Testing Journal*, **38**(4).
- Sun, L., Guo, W., Chu, J., Nie, W., Ren, Y., & Yan, S., et al. 2017. A pilot test on a membraneless vacuum preloading method. *Geotextiles & Geomembranes*.
- Wang, J., Cai, Y., Ma, J., Chu, J., Fu, H., & Wang, P., et al. 2016a. Improved vacuum preloading method for consolidation of dredged clay-slurry fill. *Journal of Geotechnical & Geoenvironmental Engineering, ASCE*, 142(11), 06016012.
- Wang, J., Ma, J., Liu, F. 2016b. Experimental study on the improvement of marine clay slurry by electroosmosis-vacuum preloading. *Geotextiles and Geomembranes*. 44:615 - 622.
- Wang, J., Ni, J., Cai, Y., Fu, H., and Wang, P. 2017. Combination of vacuum preloading and lime treatment for improvement of dredged fill. *Engineering Geology*, 227, 149-158.
- Wang J, Fu, H.T., Liu, F.Y., Cai, Y.Q., & Zhou, J. 2018a. Influence of the electro-osmosis activation time on vacuum electro-osmosis consolidation of a dredged slurry. *Canadian Geotechnical Journal*. 55(1):147-153.
- Wang, J., Cai, Y., Ni, J., Geng, X., and Xu, F. 2018b. "Effect of sand on the vacuum consolidation of dredged slurry." *Marine Georesources & Geotechnology*, 36(02), 238-244.

- Wu, H.N., Shen, S.L., Ma, L., Yin, Z.Y., and Horpibulsuk, S. 2015. Evaluation of the strength increase of marine clay under staged embankment loading: a case study, *Marine Georesources and Geotechnology*, 33(6), 532-541.
- Yoshikuni, H., & Nakanodo, H. 1974. Consolidation of soils by vertical drain wells with finite hydraulic conductivity. *Soil Found*, **14**(2), 35-46.
- Yu, X. J., & Shi, J. Y. 2009. Research on the Disturbed State Concept for Soft Clay Roadbed. *Geohunan International Conference* (pp.92-98).